

---

# EPIC: Graph Augmentation with Edit Path Interpolation via Learnable Cost

---

**Jaeseung Heo\***

Graduate School of Artificial Intelligence  
POSTECH  
South Korea  
jsheo12304@postech.ac.kr

**Seungbeom Lee\***

Graduate School of Artificial Intelligence  
POSTECH  
South Korea  
slee2020@postech.ac.kr

**Sungsoo Ahn**

Graduate School of Artificial Intelligence  
POSTECH  
South Korea  
sungsoo.ahn@postech.ac.kr

**Dongwoo Kim**

Graduate School of Artificial Intelligence  
POSTECH  
South Korea  
dongwoo.kim@postech.ac.kr

## Abstract

Graph-based models have become increasingly important in various domains, but the limited size and diversity of existing graph datasets often limit their performance. To address this issue, we propose EPIC (**E**dit **P**ath **I**nterpolation via learnable **C**ost), a novel interpolation-based method for augmenting graph datasets. Our approach leverages graph edit distance to generate new graphs that are similar to the original ones but exhibit some variation in their structures. To achieve this, we learn the graph edit distance through a comparison of labeled graphs and utilize this knowledge to create graph edit paths between pairs of original graphs. With randomly sampled graphs from a graph edit path, we enrich the training set to enhance the generalization capability of classification models. We demonstrate the effectiveness of our approach on several benchmark datasets and show that it outperforms existing augmentation methods in graph classification tasks.

## 1 Introduction

Graph data has become increasingly important in various domains, such as social networks, bioinformatics, and recommendation systems [1–3]. However, the limited size and diversity of existing graph datasets often limit the performance of graph-based models. One way to overcome this limitation is to augment the existing dataset by generating new graphs with similar properties. [4–12] The augmentation can improve the generalization ability of graph-based models and make them more robust to different real-world scenarios [13, 14].

The mixup method has proven successful as a data augmentation technique, particularly for Euclidean data such as images [7, 13, 15]. It involves generating new samples by performing linear interpolation between the features and labels of two randomly selected samples from the original dataset. This method has demonstrated its effectiveness in enhancing the generalization and robustness of deep learning models for image classification tasks [16].

However, applying the mixup method directly to graph data poses challenges. Unlike the Euclidean domain, graph structures lack a direct spatial arrangement of their elements, making it difficult

---

\*Equal contribution.

to define meaningful linear interpolations for graphs. This highlights the necessity of exploring alternative augmentation methods specifically designed for graph data.

In this paper, we propose a novel approach to graph dataset augmentation based on the concept of graph edit distance [17]. The graph edit distance is a widely-used metric that quantifies the similarity between two graphs by counting the minimum number of edit operations required to transform one graph into another, such as node and edge insertions, deletions, or substitutions. By computing the graph edit distance between two graphs, we construct a graph edit path representing the transformation process from one graph to the other through edit operations. The intermediate graph states along this path can be seen as an interpolation between two graphs and are utilized to augment the training set.

A simple count-based approach for edit distance computation, however, may not adequately capture the importance of individual operations. For instance, operations that modify functional groups in molecular graphs may hold greater significance than others [18, 19]. Hence, we introduce a problem-specific cost model to account for the context-dependent cost. We formulate an edit distance learning framework that leverages the insight that the distances between graphs within the same class should be relatively shorter than those between different classes. This enables us to learn a cost model that better reflects the underlying graph data characteristics.

By combining the graph edit distance metric with our learned cost model, we present a novel graph dataset augmentation method named Edit Path Interpolation via learnable Cost (EPIC). Experimental evaluations on various graph classification tasks demonstrate the effectiveness and improved performance of our approach compared to existing methods. Additional experiments under the presence of noisy labels show the robustness of our approach against the others.

## 2 Related Work

### 2.1 Graph edit distance

The graph edit distance is a metric that quantifies the dissimilarity between two graphs [17]. It measures the minimum number of edit operations required to transform one graph into another. These edit operations include node and edge insertion, deletion, and substitution. The computational complexity of obtaining graph edit distance is known to NP-complete [20]. A number of works addressing the problem of the high computational cost have been proposed. Cross et al. [21] cast the optimization process into a Bayesian framework with a genetic search algorithm. Myers et al. [22] adopt the Levenshtein distance to model the probability distribution for structural errors in the graph-matching. In [23], a binary linear programming formulation of the graph edit distance for unweighted, undirected graphs is proposed. Fischer et al. [24] propose an approximated graph edit distance based on Hausdorff matching. Recent approaches adopt the deep learning method to efficiently prune the search tree in computation [25].

Recently, deep neural network-based graph edit distance learning methods have been proposed. In contrast to the traditional approximation methods, where the cost of edit operation is fixed, these methods learn the cost of individual edit operations. One standard approach to learning costs using neural networks involves obtaining embeddings from node and edge attributes, which are then used to compute the edit distance in a supervised manner [26, 27]. However, these approaches require ground truth or expected correspondences between two graphs, which are inapplicable in various situations. Riba et al. [28] learn the cost using node features extracted by graph neural networks and optimizes the cost by approximating graph edit distance to Hausdorff distance. The Hausdorff distance is an effective method for approximating the graph edit distance in quadratic time, but it is not suitable for edit path construction since it allows one-to-many substitution between nodes.

### 2.2 Graph augmentation for graph neural networks

With the success of recent Graph Neural Networks (GNNs) for graph-level classification tasks, augmentation methods for graph-structured data aim to improve the generalization ability of GNNs by creating diverse training samples. Most commonly used augmentation methods are based on random modifications on original data [5, 4, 6]. For example, Dropnode [5] and DropEdge [4] uniformly drop nodes and edges, respectively. A subgraph sampling [6, 29] and motif swap [30] perturb the subgraph of the original graph via subgraph matching. These methods assign the same labels before and after the perturbation.

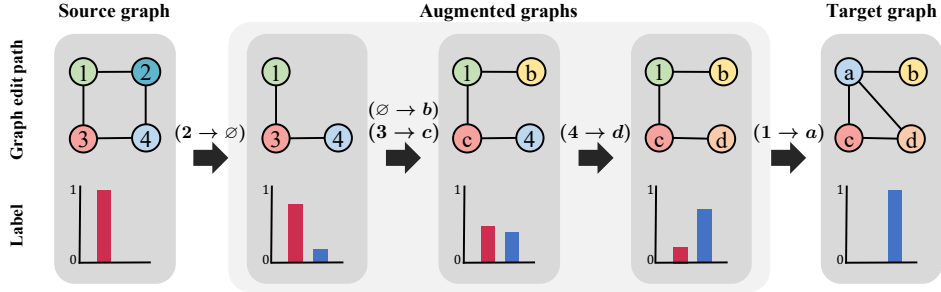


Figure 1: Illustration of graph edit path and their corresponding labels for augmentation.

To overcome the simplicity of basic approaches, mixup-based methods are proposed for graph augmentation [8, 10, 9, 12]. The mixup methods are an augmentation technique that generates new training data by taking convex combinations of pairs of inputs and their corresponding labels. Mixup methods can be naturally used for regular data, such as images. However, applying mixup for graph-structure data is challenging due to the irregular structure. Manifold mixup [8] interpolates embeddings from the last layer for two graphs and uses it as a graph representation of the augmented graph. Submix [10] proposes a node split and merge algorithm to perturb original graphs and then mix random subgraphs of multiple graphs. ifMixup [9] adds dummy nodes to match the size of two graphs. Then it interpolates between node feature matrices and adjacency matrices to generate mixed graphs. S-mixup [12] computes an alignment matrix between two graphs with graph matching network [31] first and then mixes up node features. G-mixup [11] mixes graphons [32] of different classes and augments training set by generating the graphs from the mixed graphon.

### 3 EPIC: Edit Path Interpolation via learnable Cost

In this section, we first describe a graph data augmentation method with a graph edit path. We then propose a method to learn a graph edit distance by learning the cost of individual edit operations.

#### 3.1 Augmentation with graph edit path

**Construction of graph edit path** We consider a graph  $G = (\mathcal{V}, \mathcal{E})$  associated with node and edge attributes. The graph edit distance is a metric that quantifies the dissimilarity between two graphs. It measures the minimum number of edit operations required to transform one graph into another or computes the total cost of edit operations if the cost of individual operations varies. These edit operations involve node and edge insertion, deletion, and attribute substitution.

Once the graph edit distance is computed, a graph edit path can be obtained by applying a series of edit operations from a source graph to reach a target graph. It represents the step-by-step transformation from one graph to another while minimizing the edit distance.

The graph edit distance is generally invariant to the order of edit operations. However, there are certain dependencies between node and edge operations. The node deletion operation can only be performed after all the connected edges are deleted. The edge insertion operation can only be performed when the two target nodes are presented.

We only consider the node operations in order to simplify the graph edit path construction. Specifically, when a new node is inserted into a graph, we perform edge insertion operations for all edges whose adjacent nodes are given after insertion. When a node is deleted, we perform edge deletion operations for all edges connected to the deleted node. When a node is substituted, we perform edge insertion, deletion, and substitution operations accordingly. The detailed algorithm is provided in [Algorithm 1](#). By doing so, we can construct the graph edit path whose length is equal to the number of node edit operations in the computation of the graph edit distance. [Figure 1](#) illustrates an example of a graph edit path between two graphs and possible augmentation.

**Graph augmentation and label assignment** We use the graph edit path to construct an augmented graph. We randomly sample two graphs in the training set. The graph edit distance between the two

---

**Algorithm 1** Applying node operation

---

**Require:** A node operation ( $u \rightarrow v$ ), source graph  $G_S = (\mathcal{V}_S, \mathcal{E}_S)$ , target graph  $G_T = (\mathcal{V}_T, \mathcal{E}_T)$ , and the current graph  $G_C = (\mathcal{V}_C, \mathcal{E}_C)$ .

```
1: if  $u = \emptyset$  then
2:   Insert the node  $v$  to  $\mathcal{V}_C$ .
3: else if  $v = \emptyset$  then
4:   Delete the node  $u$  from  $\mathcal{V}_C$ .
5: else
6:   Substitute the node feature of node  $u$  with the node feature of node  $v$ .
7: end if
8: for each edge  $(u, u')$  in  $\mathcal{E}_C$  do
9:   if node  $u' \in \mathcal{V}_T$  and edge  $(u, u')$  not in  $\mathcal{E}_T$  then
10:    Remove the edge  $(u, u')$  from  $\mathcal{E}_C$ .
11:   else if node  $u' \in \mathcal{V}_T$  and edge  $(v, u')$  in  $\mathcal{E}_T$  then
12:    Substitute edge attributes of  $(u, u')$  in  $\mathcal{E}_C$  with those of  $(v, u')$  in  $\mathcal{E}_T$  if needed.
13:   end if
14: end for
15: for each edge  $(v, v') \in \mathcal{E}_C$  adjacent to node  $v$  in  $\mathcal{V}_T$  do
16:   if node  $v' \in \mathcal{V}_C$  then
17:    Insert the edge  $(v, v')$  to  $\mathcal{E}_C$ .
18:   end if
19: end for
```

---

graphs is computed, then the graph edit path is constructed with node operations in random order. The samples obtained from a graph edit path are used as augmented graphs. Examples of augmented graphs are provided in Figure 1.

To assign a label to the augmented graph, we use the cost of edit operations from the augmented graph to the source and the target graphs. Let  $(o_1, \dots, o_n)$  be a sequence of edit operations applied to transforming source graph  $G_S$  to target graph  $G_T$ , and  $c(o)$  be the real-valued cost function of operation  $o$ , which is precisely defined in Section 3.2. With the corresponding one-hot classification label of the source graph  $\mathbf{y}_S$  and the target graph  $\mathbf{y}_T$ , the label of the augmented graph  $\bar{\mathbf{y}}$  obtained by applying the first  $m$  operations  $(o_1, \dots, o_m)$  is computed as

$$\bar{\mathbf{y}} = \frac{\sum_{i=m+1}^n c(o_i)}{\sum_{i=1}^n c(o_i)} \mathbf{y}_S + \frac{\sum_{i=1}^m c(o_i)}{\sum_{i=1}^n c(o_i)} \mathbf{y}_T, \quad (1)$$

where  $c(\cdot)$  measures the cost of an operation. The assigned label is inversely proportional to the operation cost to reach the source or target from the augmented graph.

### 3.2 Learning costs of edit operations

The standard unit cost model [17, 24, 33] of the graph edit distance is incapable of measuring the importance of each operation as all operations are assigned the same cost, regardless of their significance or impact. However, the importance of edit operations would differ based on the context of the dataset. For example, changes in a functional group of molecular graphs can lead to larger semantic perturbation than the other parts in a property prediction task [18, 19]. Therefore, the edit operation leading to a large semantic modification should cost more than the others. To measure the importance of each operator in the computation of graph edit distance, we propose a learning algorithm for the operation cost based on a neural network model.

**Triplet loss for learning distance** A good cost function should be problem dependent. We use the triplet loss with known labels [34] to learn the graph edit distance and the operation costs therein. We assume that the pair of graphs within the same class has a relatively shorter distance than those of different classes. Let  $\text{GED}(G, G')$  be the distance between graphs  $G$  and  $G'$ . We propose a triplet loss-based objective function to encode our intuition:

$$\mathcal{L}(G, G^+, G^-) = \max(\text{GED}(G, G^+) - \text{GED}(G, G^-) + \gamma, 0), \quad (2)$$

where  $G^+$  is a positive example whose label is the same as  $G$ ,  $G^-$  is a negative example whose labels are different from  $G$ , and  $\gamma$  is a margin hyperparameter.

**Graph edit distance as constrained optimization** The computational complexity of graph edit distance computation is NP-complete [20]. Learning graph edit distance often requires relaxation to make the algorithm tractable [24, 33]. To simplify the learning process, we assume that the cost of node operation *subsumes* the cost of dependent edit operations, similar to the construction of the edit path. With the simplified assumption, we only need to consider the following three cases when computing the edit distance between source graph  $G_S = (\mathcal{V}_S, \mathcal{E}_S)$  and target graph  $G_T = (\mathcal{V}_T, \mathcal{E}_T)$  with operation cost function  $c : \mathcal{V}_S \cup \emptyset \times \mathcal{V}_T \cup \emptyset \rightarrow \mathbb{R}$ , where  $\emptyset$  represents an empty node:

- Node  $u$  in  $\mathcal{V}_S$  is substituted by node  $v$  in  $\mathcal{V}_T$  with substitution cost  $c(u, v)$ .
- Node  $u$  in  $\mathcal{V}_S$  is deleted with deletion cost  $c(u, \emptyset)$ .
- Node  $v$  in  $\mathcal{V}_T$  is inserted with insertion cost  $c(\emptyset, v)$ .

We construct a cost matrix that encapsulates all required costs to compute the edit distance between two graphs. The cost matrix is constructed as

$$C = \begin{bmatrix} c(u_1, v_1) & \cdots & c(u_1, v_m) & c(u_1, \emptyset) & \cdots & \infty \\ \vdots & \ddots & \vdots & \vdots & \ddots & \vdots \\ c(u_n, v_1) & \cdots & c(u_n, v_m) & \infty & \cdots & c(u_n, \emptyset) \\ c(\emptyset, v_1) & \cdots & \infty & \infty & \cdots & \infty \\ \vdots & \ddots & \vdots & \vdots & \ddots & \vdots \\ \infty & \cdots & c(\emptyset, v_m) & \infty & \cdots & \infty \end{bmatrix}, \quad (3)$$

where  $n$  and  $m$  are the number of nodes in  $G_S$  and  $G_T$ , respectively.

With the cost matrix, the problem of computing the graph edit distance can be reduced to solving the assignment problem. Since the node in the source graph can only be substituted or deleted, only one operation can be performed in each of the first  $n$  rows. Similarly, since the node in the target graph can only be substituted or inserted, only one operation in each of the first  $m$  columns can be performed in edit distance computation. A binary assignment matrix  $X$ , whose size is the same as the cost matrix, is introduced to indicate which operation is performed in edit distance computation. With the assignment matrix, the computation of graph edit distance can be formulated as a constrained optimization problem

$$\begin{aligned} \text{GED}(G_S, G_T) &= \min_X \sum_{i=1}^{n+m} \sum_{j=1}^{n+m} C_{ij} X_{ij} \\ \text{s.t. } \sum_{j=1}^{n+m} X_{ij} &= 1, 1 \leq i \leq n, \quad \sum_{i=1}^{n+m} X_{ij} = 1, 1 \leq j \leq m, \quad X_{ij} \in \{0, 1\}. \end{aligned} \quad (4)$$

**Design cost function with neural networks** We introduce the graph neural network framework to parameterize the cost function  $c$ . Specifically, we use the embedding distances between two nodes as the substitution cost. Let  $h_u$  and  $h_v$  be the output embedding of node  $u \in G_S$  and  $v \in G_T$  from a graph neural network. We use the distance between two embeddings as a substitution cost, i.e.,  $c_\theta(u, v) = \|h_u - h_v\|_2$ , where  $\theta$  is the parameter of the graph neural network. The embeddings of the graph neural network encode the neighborhood structure of the target node. If the embeddings of two nodes are similar, then the two nodes are likely to play a similar role in the graph. Hence, the substitution cost measures the structural similarity between two nodes. For the insertion and deletion operations, we additionally introduce a multi-layer perceptron, i.e.,  $c_{\theta, \phi}(u, \epsilon) = \text{MLP}_\phi(h_u)$  and  $c_{\theta, \phi}(\epsilon, v) = \text{MLP}_\phi(h_v)$ , where  $\phi$  denotes the parameters of MLP. The MLP computes the cost of insertion and deletion using the embedding of a node. We use the same network for both insertion and deletion. The graph neural networks encode the local structure of nodes into node embeddings. Consequently, by considering the costs of node operations, we effectively encapsulate the information regarding the neighborhood edges as well.

**Model optimization with a differentiable assignment matrix** To learn the graph edit distance, we need to minimize the loss in Equation 2 w.r.t  $\theta$  and  $\phi$ . However, this optimization involves a non-differentiable optimization problem w.r.t the assignment matrix  $X$  in Equation 4. The Hungarian algorithm [35] can be used to find the optimal assignment  $X$  for each iteration of the stochastic

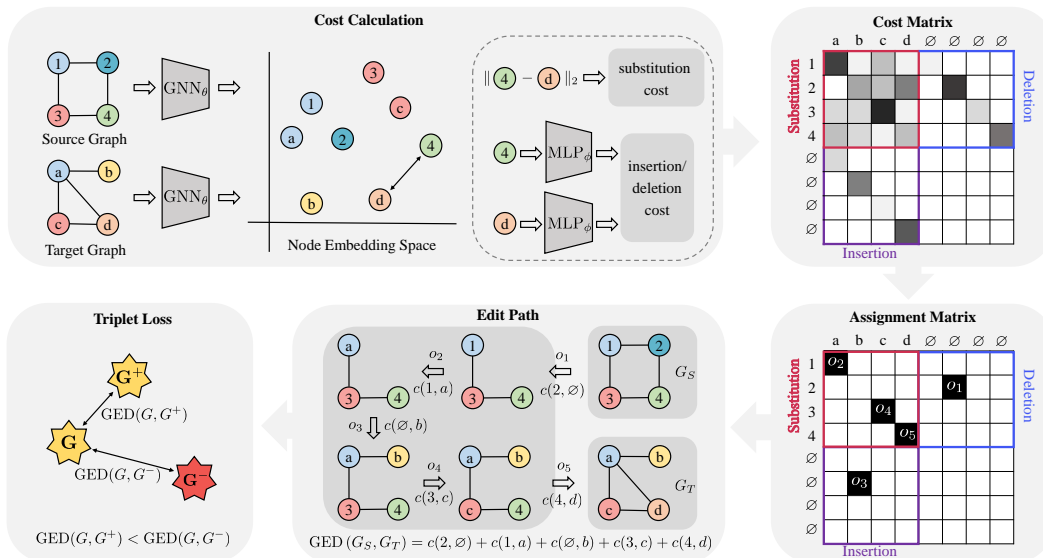


Figure 2: Overall illustration of graph edit distance learning. The assignment matrix can be obtained by either Hungarian or Sinkhorn-Knopp. For learning, we use Sinkhorn-Knopp, and for augmentation, we use Hungarian.

gradient descent step. However, the Hungarian algorithm is non-differentiable and has a computational complexity of  $O(n^3)$ , making it difficult to employ during gradient-based optimization. We instead employ the Sinkhorn-Knopp algorithm [36] to address this issue to obtain a differentiable assignment matrix. The Sinkhorn-Knopp algorithm transforms a non-negative matrix into a doubly stochastic matrix to approximate the Hungarian algorithm. Specifically, Sinkhorn-Knopp iteratively updates a soft assignment matrix  $\tilde{X}$  via two intermediate variables  $\mathbf{u}$  and  $\mathbf{v}$ . Once  $\mathbf{u}$  and  $\mathbf{v}$  are initialized as a vector of ones, i.e.,  $\mathbf{u}^{(0)} = [1, \dots, 1]^\top$ , at  $k$ -th iteration of Sinkhorn-Knopp approximates the assignment matrix via

$$\mathbf{u}^{(k)} = \frac{X^{(k-1)} \mathbf{1}}{K \mathbf{v}^{(k-1)}}, \quad \mathbf{v}^{(k)} = \frac{X^{(k-1)\top} \mathbf{1}}{K^\top \mathbf{u}^{(k-1)}}, \quad \tilde{X}^{(k)} = \text{diag}(\mathbf{u}^{(k)}) K \text{diag}(\mathbf{v}^{(k)}), \quad (5)$$

where each entry of matrix  $K$  is parameterized by the cost matrix and a regularizer parameter  $\delta$  as  $K_{ij} = \exp(-C_{ij}/\delta)$ , and  $\mathbf{1}$  is a vector of ones.  $\delta$  is a regularization term controlling the sharpness of the assignment matrix.

Note that the back-propagation algorithm needs to optimize the entire iterative process of the Sinkhorn-Knopp approximation. In experiments, we set the number of maximum iterations to 10 to reduce the computational cost. After learning the cost function, to augment a pair of randomly selected graphs, we first compute the cost matrix and then create a graph edit path using the optimal assignment from the Hungarian algorithm. Figure 2 shows the overall illustration of our proposed approach.

## 4 Experiments

In this section, we first show the effect of EPIC in graph classification tasks over 11 datasets. We further evaluate the robustness of GNNs with our method against corrupted labels. We provide additional analysis of our model selection process.

### 4.1 Effect of augmentation for graph classification

**Datasets** We used eight classification datasets: NCI1, BZR, COX2, Mutagenicity, IMDB-BINARY, IMDB-MULTI, PROTEINS, ENZYMES from TUDataset [2] and three classification dataset: BBBP, BACE, HIV from MoleculeNet [37]. The datasets cover a wide range of tasks, including social networks, bioinformatics, and molecules. The detailed statistics of each dataset are shown in Appendix A.

Table 1: Classification accuracy of TUDataset [2]. We report the average and standard deviation (in brackets) over five seeds. We mark the best and the second-best performances in **bold** and underline, respectively. The rank column shows the average rank of a model performance across all datasets.

	Method	NCI1	BZR	COX2	Mutagen.	IMDB-B	IMDB-M	PROTEINS	ENZYMES	Rank
GIN	Vanilla	81.68 <sub>(0.8)</sub>	87.07 <sub>(2.7)</sub>	83.40 <sub>(2.7)</sub>	81.57 <sub>(0.7)</sub>	72.90 <sub>(0.6)</sub>	48.40 <sub>(1.2)</sub>	67.80 <sub>(2.2)</sub>	46.33 <sub>(2.3)</sub>	<u>3.5</u>
	Dropedge [4]	74.61 <sub>(0.7)</sub>	85.85 <sub>(0.4)</sub>	80.43 <sub>(2.7)</sub>	79.13 <sub>(1.1)</sub>	71.20 <sub>(1.6)</sub>	47.20 <sub>(2.0)</sub>	68.97 <sub>(1.6)</sub>	39.00 <sub>(3.1)</sub>	5.4
	Dropnode [5]	73.05 <sub>(1.8)</sub>	85.61 <sub>(3.0)</sub>	78.51 <sub>(1.6)</sub>	77.91 <sub>(1.0)</sub>	72.90 <sub>(3.4)</sub>	46.60 <sub>(2.0)</sub>	67.53 <sub>(3.3)</sub>	38.00 <sub>(3.6)</sub>	6.1
	SubMix [10]	81.31 <sub>(0.6)</sub>	85.61 <sub>(3.6)</sub>	83.62 <sub>(2.3)</sub>	66.58 <sub>(1.5)</sub>	71.70 <sub>(1.0)</sub>	<u>48.60<sub>(1.0)</sub></u>	<u>70.76<sub>(2.2)</sub></u>	44.33 <sub>(4.8)</sub>	4.0
	M-Mix [8]	81.00 <sub>(0.4)</sub>	85.37 <sub>(3.6)</sub>	<u>84.47<sub>(1.0)</sub></u>	<u>81.68<sub>(0.9)</sub></u>	<u>73.20<sub>(0.6)</sub></u>	47.93 <sub>(1.8)</sub>	68.70 <sub>(1.1)</sub>	<u>46.67<sub>(1.7)</sub></u>	<u>3.5</u>
	G-Mix [11]	80.92 <sub>(1.9)</sub>	<b>88.05<sub>(1.6)</sub></b>	82.98 <sub>(0.8)</sub>	81.66 <sub>(0.6)</sub>	72.20 <sub>(1.0)</sub>	48.13 <sub>(1.2)</sub>	68.16 <sub>(2.8)</sub>	43.67 <sub>(6.9)</sub>	4.1
	EPIC	<b>82.31<sub>(1.5)</sub></b>	<u>87.32<sub>(2.0)</sub></u>	<b>84.89<sub>(2.7)</sub></b>	<b>81.86<sub>(1.0)</sub></b>	<b>73.40<sub>(0.8)</sub></b>	<b>48.93<sub>(0.6)</sub></b>	<b>70.85<sub>(0.9)</sub></b>	<b>47.83<sub>(3.5)</sub></b>	<b>1.1</b>
GCN	Vanilla	81.07 <sub>(0.7)</sub>	85.85 <sub>(2.8)</sub>	84.26 <sub>(2.2)</sub>	81.70 <sub>(1.1)</sub>	<u>70.60<sub>(1.3)</sub></u>	<b>48.27<sub>(1.5)</sub></b>	64.13 <sub>(1.6)</sub>	44.67 <sub>(5.7)</sub>	3.5
	Dropedge [4]	74.24 <sub>(1.0)</sub>	82.93 <sub>(4.3)</sub>	83.40 <sub>(1.2)</sub>	80.37 <sub>(0.6)</sub>	70.50 <sub>(1.8)</sub>	45.67 <sub>(1.5)</sub>	64.75 <sub>(3.4)</sub>	39.33 <sub>(1.8)</sub>	5.4
	Dropnode [5]	73.78 <sub>(1.8)</sub>	80.73 <sub>(2.4)</sub>	79.15 <sub>(1.8)</sub>	78.32 <sub>(1.6)</sub>	69.40 <sub>(3.0)</sub>	39.80 <sub>(3.7)</sub>	<b>68.43<sub>(1.8)</sub></b>	36.17 <sub>(3.6)</sub>	6.0
	SubMix [10]	81.99 <sub>(0.6)</sub>	86.34 <sub>(2.0)</sub>	83.62 <sub>(4.1)</sub>	79.77 <sub>(0.9)</sub>	68.50 <sub>(0.1)</sub>	46.47 <sub>(2.5)</sub>	66.82 <sub>(2.1)</sub>	43.67 <sub>(4.9)</sub>	4.5
	M-Mix [8]	81.41 <sub>(0.5)</sub>	84.15 <sub>(2.3)</sub>	83.83 <sub>(2.1)</sub>	<u>81.96<sub>(0.6)</sub></u>	69.40 <sub>(1.1)</sub>	46.40 <sub>(2.7)</sub>	66.28 <sub>(1.5)</sub>	44.00 <sub>(5.3)</sub>	4.1
	G-Mix [11]	<u>82.04<sub>(1.8)</sub></u>	<u>87.32<sub>(2.4)</sub></u>	<u>84.89<sub>(1.4)</sub></u>	80.32 <sub>(0.7)</sub>	69.90 <sub>(1.8)</sub>	45.87 <sub>(3.0)</sub>	<u>68.07<sub>(1.2)</sub></u>	<u>46.17<sub>(4.3)</sub></u>	<u>3.0</u>
	EPIC	<b>82.31<sub>(0.1)</sub></b>	<b>87.80<sub>(1.2)</sub></b>	<b>85.74<sub>(0.6)</sub></b>	<b>82.19<sub>(0.5)</sub></b>	<b>70.80<sub>(1.7)</sub></b>	<u>47.07<sub>(1.4)</sub></u>	67.44 <sub>(1.2)</sub>	<b>47.17<sub>(5.6)</sub></b>	<b>1.4</b>

**Baselines** For baseline augmentation models, we employ two classical graph augmentation methods: DropEdge [4] and DropNode [5], and three Mixup-based augmentations: SubMix [10], Manifold-Mixup (M-Mixup) [8], and G-Mixup [11]. We also report the performance of a vanilla model without augmentation.

**Implementation details** We first learn the cost of edit operations for each dataset. We use Adam optimizer [38] with a learning rate decay of 0.1 every 25 epochs. We train the cost function for 100 epochs on TUDataset. While we use Sinkhorn-Knopp approximation with  $k = 10$  in Equation 5 for training, the Hungarian algorithm is used for inference to obtain an optimal assignment given costs. We perform graph classification tasks with GIN [39] and GCN [40] as a backbone model for augmentation. When we train each backbone model, we use the same hyperparameter and architecture for all baselines and our method for a fair comparison. We follow the Open Graph Benchmark setting [1] for MoleculeNet dataset. When training classification models, we compute the edit path between randomly paired graphs in each batch and use randomly chosen graphs from the edit path as augmentation. We use the validation set to choose the portion of augmented data points.

The additional details of hyperparameters and model configurations can be found in Appendix B.

**Classification results** Table 1 shows the overall results of the TUDataset for graph classification tasks. Our augmentation method outperforms the other baselines on seven and six datasets with GIN and GCN backbones, respectively, and achieves the second-best performance on one dataset with GIN and GCN backbones. Table 2 shows the classification AUC-ROC with MoleculeNet datasets. The results show that EPIC consistently improves classification accuracy over the vanilla model, whereas the other augmentations occasionally degrade the classification performance.

Table 2: Classification AUC-ROC of MoleculeNet [37].

	Method	BBBP	BACE	HIV	Rank
GIN	Vanilla	<u>65.90<sub>(1.9)</sub></u>	77.01 <sub>(2.7)</sub>	75.10 <sub>(2.7)</sub>	4.0
	Dropedge [4]	65.32 <sub>(1.8)</sub>	74.50 <sub>(0.9)</sub>	75.57 <sub>(0.6)</sub>	4.7
	Dropnode [5]	64.32 <sub>(5.0)</sub>	76.37 <sub>(3.0)</sub>	75.36 <sub>(1.3)</sub>	5.3
	SubMix [10]	65.58 <sub>(5.0)</sub>	75.26 <sub>(6.8)</sub>	<u>76.36<sub>(1.3)</sub></u>	<u>3.7</u>
	M-Mix [8]	64.48 <sub>(1.6)</sub>	75.30 <sub>(2.6)</sub>	75.55 <sub>(2.0)</sub>	4.7
	G-Mix [11]	64.33 <sub>(3.2)</sub>	<b>78.54<sub>(1.9)</sub></b>	75.29 <sub>(0.6)</sub>	4.3
	EPIC	<b>68.33<sub>(1.9)</sub></b>	<u>77.17<sub>(3.2)</sub></u>	<b>76.85<sub>(1.4)</sub></b>	<b>1.3</b>
GCN	Vanilla	66.08 <sub>(3.4)</sub>	76.35 <sub>(4.2)</sub>	75.45 <sub>(0.7)</sub>	4.7
	Dropedge [4]	65.71 <sub>(2.5)</sub>	72.79 <sub>(7.9)</sub>	75.90 <sub>(1.6)</sub>	5.0
	Dropnode [5]	<u>68.33<sub>(3.0)</sub></u>	71.37 <sub>(5.0)</sub>	74.41 <sub>(0.9)</sub>	5.3
	SubMix [10]	67.68 <sub>(1.2)</sub>	75.19 <sub>(5.6)</sub>	75.61 <sub>(2.1)</sub>	4.0
	M-Mix [8]	67.38 <sub>(2.0)</sub>	<b>79.67<sub>(0.9)</sub></b>	75.23 <sub>(1.2)</sub>	<u>3.7</u>
	G-Mix [11]	65.10 <sub>(2.3)</sub>	77.54 <sub>(5.3)</sub>	<u>75.99<sub>(0.9)</sub></u>	4.0
	EPIC	<b>68.68<sub>(2.3)</sub></b>	<u>77.67<sub>(1.7)</sub></u>	<b>76.81<sub>(1.3)</sub></b>	<b>1.3</b>

Table 3: Robustness analysis on IMDB-BINARY, IMDB-MULTI, and Mutagenicity datasets. We randomly corrupt the label of the training set and measure the test performance with random noise.

Method	IMDB-BINARY			IMDB-MULTI			Mutagenicity		
	20%	40%	60%	20%	40%	60%	20%	40%	60%
Vanilla	72.50 <sub>(1.2)</sub>	66.10 <sub>(1.6)</sub>	44.30 <sub>(6.6)</sub>	48.00 <sub>(1.2)</sub>	46.07 <sub>(1.1)</sub>	42.33 <sub>(3.7)</sub>	75.30 <sub>(0.7)</sub>	68.52 <sub>(1.4)</sub>	46.38 <sub>(3.1)</sub>
Dropedge [4]	70.30 <sub>(4.1)</sub>	66.20 <sub>(5.1)</sub>	48.30 <sub>(4.0)</sub>	44.80 <sub>(2.4)</sub>	42.60 <sub>(3.1)</sub>	37.93 <sub>(2.2)</sub>	75.47 <sub>(0.9)</sub>	67.71 <sub>(1.5)</sub>	45.13 <sub>(4.1)</sub>
Dropnode [5]	70.90 <sub>(1.0)</sub>	68.80 <sub>(3.4)</sub>	52.40 <sub>(2.3)</sub>	45.60 <sub>(1.9)</sub>	43.00 <sub>(2.5)</sub>	39.53 <sub>(1.9)</sub>	72.98 <sub>(1.5)</sub>	66.26 <sub>(1.5)</sub>	45.89 <sub>(3.1)</sub>
SubMix [10]	72.20 <sub>(1.0)</sub>	67.70 <sub>(2.0)</sub>	43.10 <sub>(9.4)</sub>	48.67 <sub>(1.2)</sub>	45.53 <sub>(1.3)</sub>	40.60 <sub>(5.2)</sub>	73.00 <sub>(1.5)</sub>	66.86 <sub>(2.6)</sub>	<b>59.03</b> <sub>(2.5)</sub>
ManifoldMix [8]	71.90 <sub>(1.1)</sub>	69.90 <sub>(3.8)</sub>	49.70 <sub>(6.5)</sub>	48.07 <sub>(1.3)</sub>	46.67 <sub>(1.1)</sub>	43.40 <sub>(3.3)</sub>	75.49 <sub>(0.9)</sub>	67.43 <sub>(3.6)</sub>	45.91 <sub>(2.7)</sub>
G-Mix [11]	71.60 <sub>(1.9)</sub>	70.00 <sub>(4.3)</sub>	44.60 <sub>(10.0)</sub>	47.33 <sub>(0.8)</sub>	44.80 <sub>(2.1)</sub>	40.67 <sub>(1.7)</sub>	76.06 <sub>(1.5)</sub>	69.25 <sub>(0.8)</sub>	45.27 <sub>(4.1)</sub>
EPIC	<b>72.60</b> <sub>(1.1)</sub>	<b>71.00</b> <sub>(1.8)</sub>	<b>53.70</b> <sub>(3.4)</sub>	<b>49.07</b> <sub>(1.2)</sub>	<b>47.60</b> <sub>(1.1)</sub>	<b>43.73</b> <sub>(1.9)</sub>	<b>76.96</b> <sub>(1.5)</sub>	<b>69.62</b> <sub>(1.1)</sub>	49.25 <sub>(3.6)</sub>

Table 4: Comparisons between three different cost functions. Three different cost functions: unit, feature-distance, and EPIC, are tested on TUDataset. GIN is used as a backbone.

(a) Classification accuracy with augmentation

Method	NCII $\uparrow$	BZR $\uparrow$	COX2 $\uparrow$	Mutagen. $\uparrow$	PROTEINS $\uparrow$	ENZYMES $\uparrow$	IMDB-B $\uparrow$	IMDB-M $\uparrow$
Unit cost	82.28 <sub>(0.9)</sub>	86.59 <sub>(1.9)</sub>	84.47 <sub>(1.0)</sub>	81.47 <sub>(0.8)</sub>	72.80 <sub>(0.3)</sub>	48.53 <sub>(1.2)</sub>	70.49 <sub>(1.2)</sub>	46.50 <sub>(1.5)</sub>
Feature-distance	81.65 <sub>(1.4)</sub>	85.37 <sub>(1.5)</sub>	83.83 <sub>(1.2)</sub>	81.73 <sub>(0.4)</sub>	73.10 <sub>(0.7)</sub>	<b>48.93</b> <sub>(0.5)</sub>	69.96 <sub>(1.2)</sub>	46.17 <sub>(2.7)</sub>
EPIC	<b>82.31</b> <sub>(1.4)</sub>	<b>87.32</b> <sub>(2.0)</sub>	<b>84.89</b> <sub>(2.6)</sub>	<b>81.86</b> <sub>(0.9)</sub>	<b>73.40</b> <sub>(0.7)</sub>	<b>48.93</b> <sub>(0.5)</sub>	<b>70.85</b> <sub>(0.9)</sub>	<b>47.83</b> <sub>(3.5)</sub>

(b) Distance-based classification accuracy

Method	NCII $\uparrow$	BZR $\uparrow$	COX2 $\uparrow$	Mutagen. $\uparrow$	PROTEINS $\uparrow$	ENZYMES $\uparrow$	IMDB-B $\uparrow$	IMDB-M $\uparrow$
Unit cost	60.49 <sub>(0.4)</sub>	72.20 <sub>(3.7)</sub>	52.34 <sub>(3.8)</sub>	56.69 <sub>(2.0)</sub>	56.86 <sub>(1.5)</sub>	<b>25.83</b> <sub>(3.0)</sub>	55.50 <sub>(2.8)</sub>	36.33 <sub>(2.2)</sub>
Feature-distance	60.70 <sub>(0.8)</sub>	72.93 <sub>(4.0)</sub>	52.55 <sub>(3.2)</sub>	55.51 <sub>(1.8)</sub>	<b>57.31</b> <sub>(1.7)</sub>	<b>25.83</b> <sub>(2.9)</sub>	56.00 <sub>(2.8)</sub>	36.20 <sub>(1.6)</sub>
EPIC	<b>72.69</b> <sub>(0.3)</sub>	<b>77.80</b> <sub>(2.9)</sub>	<b>60.43</b> <sub>(3.5)</sub>	<b>75.33</b> <sub>(1.0)</sub>	56.95 <sub>(0.8)</sub>	23.67 <sub>(4.7)</sub>	<b>67.70</b> <sub>(1.8)</sub>	<b>39.33</b> <sub>(2.8)</sub>

## 4.2 Robustness analysis

We conduct a study that shows the robustness of the augmentation method with the presence of noisy labels. A similar study is also conducted in Hendrycks et al. [13], Pang et al. [14]. We randomly corrupt labels in the training set of IMDB-BINARY, IMDB-MULTI, and Mutagenicity datasets and test the model performance with the uncorrupted test set. We run the experiments with three different proportions of noise:  $\{0.2, 0.4, 0.6\}$  based on GIN. Except for the noise, we use the same setting used in Section 4.1. Table 3 shows the classification accuracy with different proportions of noisy labels. EPIC outperforms the other baseline models, except for one case, showing the robustness of our augmentation under the noisy environment.

## 4.3 Ablation studies

In this subsection, we show the result of ablation studies on each component in EPIC. Further ablation studies are shown in Appendix C.

**Cost function variations** We test the effectiveness of the learnable cost function against other variations of the cost function. We use two variations of the cost function: unit cost, which measures the number of edit operations, and feature-distance cost, which measures the distance between two input node features, adopted from Ling et al. [12].

The result in Table 4a shows that the learnable cost outperforms the other cost functions across all datasets. The results empirically verify our claim that the good cost function should be problem dependent and can be learned from the dataset.

We also classify the graphs in the test dataset based on their distance to the closest graph in each class. If the cost is learned properly, the distance from a test graph to the graph in the same class should be close to each other. Table 4b shows the result of distance-based classification. In most cases, EPIC outperforms the other fixed-cost methods. For some datasets, such as IMDB-BINARY, the distance-based classification performs similarly to the classification model with augmentation.



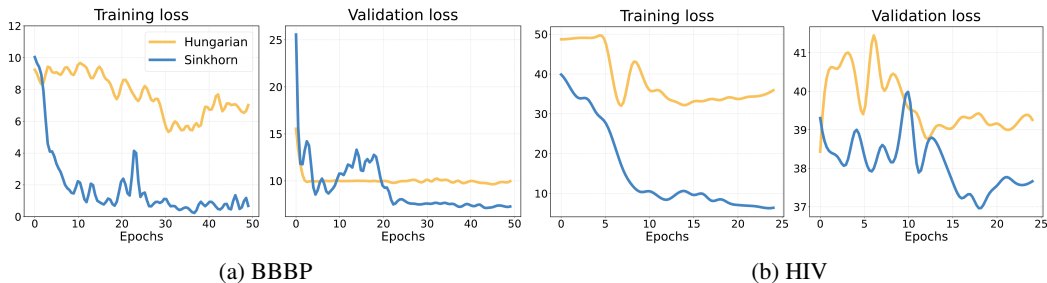


Figure 3: Training and validation loss curves on BBBP and HIV datasets with Hungarian and Sinkhorn-Knopp algorithms in the training process.

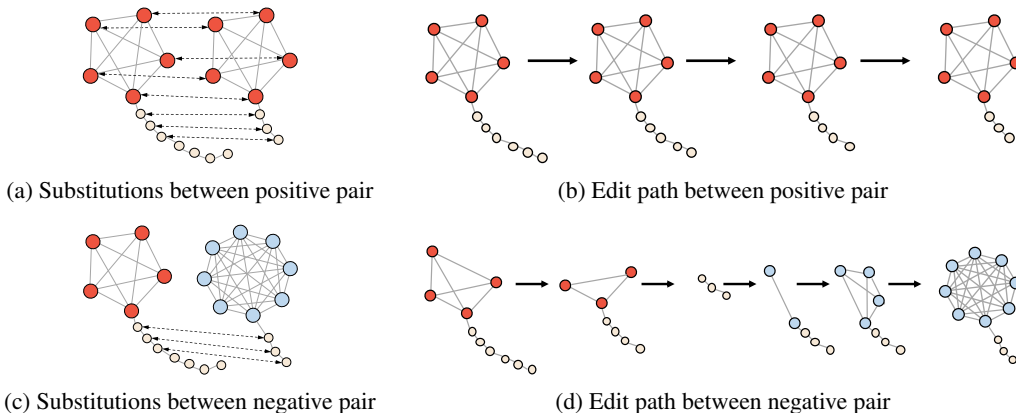


Figure 4: Examples of learned edit distance from a lollipop dataset. The dashed lines in (a) and (c) represent the nodes with substitution operations. The head nodes are substituted to their counterpart in the positive pair case, whereas no substitution is performed between the heads of the negative pair. (b) and (d) show the sampled edit path from the source to target graphs. The lollipop head remains the same during the transition with a positive pair.

**Hungarian vs Sinkhorn-Knopp** We investigate the impact of a differentiable assignment matrix with the Sinkhorn-Knopp algorithm against a fixed assignment matrix from the Hungarian algorithm in the process of training. In Figure 3, we present the training and validation curve on the BBBP and HIV datasets. In general, the Sinkhorn-Knopp algorithm shows a more stable learning process than the Hungarian algorithm. The training loss with Hungarian has not been stabilized after 40 epochs in BBBP and 20 epochs in HIV datasets. Moreover, the validation loss of Sinkhorn-Knopp is consistently lower than Hungarian after certain iterations. We conjecture that the non-smooth loss surface of Hungarian makes the gradient descent work hard, and eventually, the model fails to reach a good local minimum, whereas the smooth loss surface of Sinkhorn-Knopp results in a better performance despite being an approximation of Hungarian.

#### 4.4 Qualitative analysis

To examine how the results of the learned distance are reflected in the augmented graph, we conduct an experiment with a lollipop dataset whose structural properties are easily visualized. The  $(m, n)$ -lollipop graph consists of a head, a complete graph with  $m$  nodes, and a tail, a chain structured  $n$  nodes. The lollipop dataset consists of graphs with varying  $m$  and  $n$ . The label of a graph is the size of the head, i.e.,  $m$ . Figure 4 displays examples of the trained graph edit distances and the corresponding edit path for positive and negative pairs. With a positive pair, the learned graph edit distance substitutes the head nodes from the source graph for those of the target graph. Eventually, it maintains the complete subgraph of the head along the edit path. Whereas with a negative pair, the head nodes of the source graph are deleted first, and those of the target graph are inserted later. We also observe that the insertion and deletion costs of head nodes are more expensive than those of tail nodes, making the distance between the negative pair long. Additionally, we present the assigned

cost for substitution to each node in [Appendix D](#), which consistently shows the effectiveness of the cost function for EPIC.

## 5 Conclusion

In this paper, we have presented a novel approach for graph dataset augmentation based on the graph edit distance. Our method overcomes the limitations of linear interpolation techniques in the non-Euclidean domain and provides a tailored augmentation solution for graph data. Through extensive experiments on benchmark datasets, we have demonstrated the effectiveness of our approach in improving the performance and robustness of graph-based models. In this work, we only consider the node operation cost for computational simplicity, but incorporating edge operation cost into the framework would be a solid and important future direction.

## References

- [1] Weihua Hu, Matthias Fey, Marinka Zitnik, Yuxiao Dong, Hongyu Ren, Bowen Liu, Michele Catasta, and Jure Leskovec. Open graph benchmark: Datasets for machine learning on graphs. *Advances in neural information processing systems*, 33:22118–22133, 2020. [1](#), [7](#), [14](#), [15](#)
- [2] Christopher Morris, Nils M. Kriege, Franka Bause, Kristian Kersting, Petra Mutzel, and Marion Neumann. Tudataset: A collection of benchmark datasets for learning with graphs. In *ICML 2020 Workshop on Graph Representation Learning and Beyond (GRL+ 2020)*, 2020. URL [www.graphlearning.io](http://www.graphlearning.io). [6](#), [7](#), [14](#)
- [3] Jure Leskovec, Lada A Adamic, and Bernardo A Huberman. The dynamics of viral marketing. *ACM Transactions on the Web (TWEB)*, 1(1):5–es, 2007. [1](#)
- [4] Yu Rong, Wenbing Huang, Tingyang Xu, and Junzhou Huang. Dropedge: Towards deep graph convolutional networks on node classification. *arXiv preprint arXiv:1907.10903*, 2019. [1](#), [2](#), [7](#), [8](#), [15](#)
- [5] Wenzheng Feng, Jie Zhang, Yuxiao Dong, Yu Han, Huanbo Luan, Qian Xu, Qiang Yang, Evgeny Kharlamov, and Jie Tang. Graph random neural networks for semi-supervised learning on graphs. *Advances in neural information processing systems*, 33:22092–22103, 2020. [2](#), [7](#), [8](#)
- [6] Yuning You, Tianlong Chen, Yongduo Sui, Ting Chen, Zhangyang Wang, and Yang Shen. Graph contrastive learning with augmentations. *Advances in neural information processing systems*, 33:5812–5823, 2020. [2](#)
- [7] Hongyi Zhang, Moustapha Cisse, Yann N Dauphin, and David Lopez-Paz. mixup: Beyond empirical risk minimization. *arXiv preprint arXiv:1710.09412*, 2017. [1](#)
- [8] Vikas Verma, Alex Lamb, Christopher Beckham, Amir Najafi, Ioannis Mitliagkas, David Lopez-Paz, and Yoshua Bengio. Manifold mixup: Better representations by interpolating hidden states. In *International conference on machine learning*, pages 6438–6447. PMLR, 2019. [3](#), [7](#), [8](#)
- [9] Hongyu Guo and Yongyi Mao. ifmixup: Towards intrusion-free graph mixup for graph classification. *arXiv e-prints*, pages arXiv–2110, 2021. [3](#)
- [10] Jaemin Yoo, Sooyeon Shim, and U Kang. Model-agnostic augmentation for accurate graph classification. In *Proceedings of the ACM Web Conference 2022*, pages 1281–1291, 2022. [3](#), [7](#), [8](#)
- [11] Xiaotian Han, Zhimeng Jiang, Ninghao Liu, and Xia Hu. G-mixup: Graph data augmentation for graph classification. In *International Conference on Machine Learning*, pages 8230–8248. PMLR, 2022. [3](#), [7](#), [8](#), [15](#)
- [12] Hongyi Ling, Zhimeng Jiang, Meng Liu, Shuiwang Ji, and Na Zou. Graph mixup with soft alignments. [1](#), [3](#), [8](#), [15](#)
- [13] Dan Hendrycks, Norman Mu, Ekin D Cubuk, Barret Zoph, Justin Gilmer, and Balaji Lakshminarayanan. Augmix: A simple data processing method to improve robustness and uncertainty. *arXiv preprint arXiv:1912.02781*, 2019. [1](#), [8](#)

- [14] Tianyu Pang, Kun Xu, and Jun Zhu. Mixup inference: Better exploiting mixup to defend adversarial attacks. *arXiv preprint arXiv:1909.11515*, 2019. 1, 8
- [15] Zhiqiang Shen, Zechun Liu, Zhuang Liu, Marios Savvides, Trevor Darrell, and Eric Xing. Unmix: Rethinking image mixtures for unsupervised visual representation learning. In *Proceedings of the AAAI Conference on Artificial Intelligence*, volume 36, pages 2216–2224, 2022. 1
- [16] Sunil Thulasidasan, Gopinath Chennupati, Jeff A Bilmes, Tanmoy Bhattacharya, and Sarah Michalak. On mixup training: Improved calibration and predictive uncertainty for deep neural networks. *Advances in Neural Information Processing Systems*, 32, 2019. 1
- [17] Julian R Ullmann. An algorithm for subgraph isomorphism. *Journal of the ACM (JACM)*, 23(1):31–42, 1976. 2, 4
- [18] Joseph L Durant, Burton A Leland, Douglas R Henry, and James G Nourse. Reoptimization of mdl keys for use in drug discovery. *Journal of chemical information and computer sciences*, 42(6):1273–1280, 2002. 2, 4
- [19] Shichang Zhang, Ziniu Hu, Arjun Subramonian, and Yizhou Sun. Motif-driven contrastive learning of graph representations. *arXiv preprint arXiv:2012.12533*, 2020. 2, 4
- [20] Zeina Abu-Aisheh, Romain Raveaux, Jean-Yves Ramel, and Patrick Martineau. An exact graph edit distance algorithm for solving pattern recognition problems. In *4th International Conference on Pattern Recognition Applications and Methods 2015*, 2015. 2, 5
- [21] Andrew DJ Cross, Richard C Wilson, and Edwin R Hancock. Inexact graph matching using genetic search. *Pattern Recognition*, 30(6):953–970, 1997. 2
- [22] Richard Myers, RC Wison, and Edwin R Hancock. Bayesian graph edit distance. *IEEE Transactions on Pattern Analysis and Machine Intelligence*, 22(6):628–635, 2000. 2
- [23] Derek Justice and Alfred Hero. A binary linear programming formulation of the graph edit distance. *IEEE Transactions on Pattern Analysis and Machine Intelligence*, 28(8):1200–1214, 2006. 2
- [24] Andreas Fischer, Ching Y Suen, Volkmar Frinken, Kaspar Riesen, and Horst Bunke. Approximation of graph edit distance based on hausdorff matching. *Pattern Recognition*, 48(2):331–343, 2015. 2, 4, 5
- [25] Runzhong Wang, Tianqi Zhang, Tianshu Yu, Junchi Yan, and Xiaokang Yang. Combinatorial learning of graph edit distance via dynamic embedding. In *Proceedings of the IEEE/CVF Conference on Computer Vision and Pattern Recognition*, pages 5241–5250, 2021. 2
- [26] Xavier Cortés, Donatello Conte, and Hubert Cardot. Learning edit cost estimation models for graph edit distance. *Pattern Recognition Letters*, 125:256–263, 2019. 2
- [27] Tibério S Caetano, Julian J McAuley, Li Cheng, Quoc V Le, and Alex J Smola. Learning graph matching. *IEEE transactions on pattern analysis and machine intelligence*, 31(6):1048–1058, 2009. 2
- [28] Pau Riba, Andreas Fischer, Josep Lladós, and Alicia Fornés. Learning graph edit distance by graph neural networks. *Pattern Recognition*, 120:108132, 2021. 2
- [29] Yiwei Wang, Wei Wang, Yuxuan Liang, Yujun Cai, and Bryan Hooi. Graphcrop: Subgraph cropping for graph classification. *arXiv preprint arXiv:2009.10564*, 2020. 2
- [30] Jiajun Zhou, Jie Shen, and Qi Xuan. Data augmentation for graph classification. In *Proceedings of the 29th ACM International Conference on Information & Knowledge Management*, pages 2341–2344, 2020. 2
- [31] Yujia Li, Chenjie Gu, Thomas Dullien, Oriol Vinyals, and Pushmeet Kohli. Graph matching networks for learning the similarity of graph structured objects. In *International conference on machine learning*, pages 3835–3845. PMLR, 2019. 3

- [32] Edo M Airoidi, Thiago B Costa, and Stanley H Chan. Stochastic blockmodel approximation of a graphon: Theory and consistent estimation. *Advances in Neural Information Processing Systems*, 26, 2013. 3
- [33] Kaspar Riesen and Horst Bunke. Approximate graph edit distance computation by means of bipartite graph matching. *Image and Vision computing*, 27(7):950–959, 2009. 4, 5
- [34] Florian Schroff, Dmitry Kalenichenko, and James Philbin. Facenet: A unified embedding for face recognition and clustering. In *Proceedings of the IEEE conference on computer vision and pattern recognition*, pages 815–823, 2015. 4
- [35] Harold W Kuhn. The hungarian method for the assignment problem. *Naval research logistics quarterly*, 2(1-2):83–97, 1955. 5
- [36] Richard Sinkhorn and Paul Knopp. Concerning nonnegative matrices and doubly stochastic matrices. *Pacific Journal of Mathematics*, 21(2):343–348, 1967. 6
- [37] Zhenqin Wu, Bharath Ramsundar, Evan N Feinberg, Joseph Gomes, Caleb Geniesse, Aneesh S Pappu, Karl Leswing, and Vijay Pande. Moleculenet: a benchmark for molecular machine learning. *Chemical science*, 9(2):513–530, 2018. 6, 7, 14
- [38] Diederik P Kingma and Jimmy Ba. Adam: A method for stochastic optimization. *arXiv preprint arXiv:1412.6980*, 2014. 7
- [39] Keyulu Xu, Weihua Hu, Jure Leskovec, and Stefanie Jegelka. How powerful are graph neural networks? *arXiv preprint arXiv:1810.00826*, 2018. 7
- [40] Thomas N Kipf and Max Welling. Semi-supervised classification with graph convolutional networks. *arXiv preprint arXiv:1609.02907*, 2016. 7
- [41] David Weininger. Smiles, a chemical language and information system. 1. introduction to methodology and encoding rules. *Journal of chemical information and computer sciences*, 1988. 14
- [42] Ines Filipa Martins, Ana L Teixeira, Luis Pinheiro, and Andre O Falcao. A bayesian approach to in silico blood-brain barrier penetration modeling. *Journal of chemical information and modeling*, 52(6):1686–1697, 2012. 14
- [43] Govindan Subramanian, Bharath Ramsundar, Vijay Pande, and Rajiah Aldrin Denny. Computational modeling of  $\beta$ -secretase 1 (bace-1) inhibitors using ligand based approaches. *Journal of chemical information and modeling*, 56(10):1936–1949, 2016. 14
- [44] DTP DTP. Aids antiviral screen (2004). URL <http://dtp.nci.nih.gov/docs/aids/aids-data.html>. 14
- [45] Nikil Wale, Ian A Watson, and George Karypis. Comparison of descriptor spaces for chemical compound retrieval and classification. *Knowledge and Information Systems*, 14:347–375, 2008. 14
- [46] Pierre Mahé and Jean-Philippe Vert. Graph kernels based on tree patterns for molecules. *Machine learning*, 75(1):3–35, 2009. 14
- [47] Asim Kumar Debnath, Rosa L Lopez de Compadre, Gargi Debnath, Alan J Shusterman, and Corwin Hansch. Structure-activity relationship of mutagenic aromatic and heteroaromatic nitro compounds. correlation with molecular orbital energies and hydrophobicity. *Journal of medicinal chemistry*, 34(2):786–797, 1991. 14
- [48] Benedek Rozemberczki, Oliver Kiss, and Rik Sarkar. An api oriented open-source python framework for unsupervised learning on graphs. *arXiv preprint arXiv:2003.04819*, 10 (3340531.3412757), 2020. 14
- [49] Paul D Dobson and Andrew J Doig. Distinguishing enzyme structures from non-enzymes without alignments. *Journal of molecular biology*, 330(4):771–783, 2003. 14

- [50] Ida Schomburg, Antje Chang, Christian Ebeling, Marion Gremse, Christian Heldt, Gregor Huhn, and Dietmar Schomburg. Brenda, the enzyme database: updates and major new developments. *Nucleic acids research*, 32(suppl\_1):D431–D433, 2004. [14](#)
- [51] Rémi Flamary, Nicolas Courty, Alexandre Gramfort, Mokhtar Z Alaya, Aurélie Boisbunon, Stanislas Chambon, Laetitia Chapel, Adrien Corenflos, Kilian Fatras, Nemo Fournier, et al. Pot: Python optimal transport. *The Journal of Machine Learning Research*, 22(1):3571–3578, 2021. [15](#)

## A Dataset Details

**Dataset statistics** We present the statistics for each dataset from TUDataset [2] and MoleculeNet [37] in Table 5. It includes the number of data, classes, average nodes, and edges, the source of data, and the presence of node and edge labels. For BBBP, BACE, and HIV datasets, we use OGB package [1] to convert SMILES strings [41], the sequence of atoms and symbols, to molecular graphs.

Table 5: Statistics for each dataset from TUDataset [2] and MoleculeNet [37].

Dataset	Size	Classes	Source	Avg.nodes	Avg.edges	Node labels	Edge labels
BBBP [42]	2039	2	Small molecule	24.06	51.91	✓	✓
BACE [43]	25	2	Small molecule	34.09	73.72	✓	✓
HIV [44]	41127	2	Small molecule	25.51	54.94	✓	✓
NCI1 [45]	4110	2	Small molecule	29.87	32.30	✓	✗
BZR [46]	405	2	Small molecule	35.75	38.36	✓	✗
COX2 [46]	467	2	Small molecule	41.22	43.45	✓	✗
Mutagenicity [47]	4337	2	Small molecule	30.32	30.77	✓	✗
IMDB-BINARY [48]	1000	2	Ego network	19.77	96.53	✗	✗
IMDB-MULTI [48]	1500	3	Ego network	13.00	65.94	✗	✗
PROTEINS [49]	1113	2	Macro molecule	39.06	72.82	✓	✗
ENZYMES [50]	600	6	Macro molecule	32.63	62.14	✓	✗

**Dataset description** We use 10 graph-level classification datasets: BBBP, BACE, HIV from MoleculeNet [37] and NCI1, BZR, COX2, Mutagenicity, IMDB-BINARY, IMDB-MULTI, PROTEINS, ENZYMES from TUDataset [2]. The details of each dataset are shown in Table 6. Through the various dataset from a wide range of domains, we can test the effect of our EPIC for graph classification.

Table 6: Detailed description for each dataset from TUDataset [2] and MoleculeNet [37]

Dataset	Description
BBBP	Binary classification to predict blood-brain barrier penetration of given molecule
BACE	Binary classification to predict binding results for a set of inhibitors of human $\beta$ -secretase 1 of a given molecule
HIV	Binary classification to predict experimentally measured abilities to inhibit HIV replication
NCI1	Binary classification to predict bio-assays result to suppress the growth of human non-small cell lung cancer.
BZR	Binary classification to predict ligands for the benzodiazepine receptor
COX2	Binary classification to predict cyclooxygenase-2 Inhibitors
Mutagenicity	Binary classification to predict mutagenic bio-active compounds
IMDB-BINARY (MULTI)	Binary (Multi) classification to predict the genre of ego network derived from actor collaboration
PROTEINS	Multiclass classification to predict whether a protein is an enzyme
ENZYMES	Multiclass classification to assign enzymes to one of the 6 classes, which reflect the catalyzed chemical reaction

## B Experiment Settings

**Dataset split** To evaluate the performance of TUDataset, we split the dataset into the train, validation, and test sets using the ratio of 7:1:2. To address the issue of imbalanced labels within the dataset, we make each split has the same proportion of labels. We use the split provided by the Open Graph Benchmark [1] to evaluate the performance of the MoleculeNet dataset. The same split is used for all experiments.

**Training cost function** To train the cost function using the triplet loss, we randomly sample a positive sample and a negative sample from the dataset. On each epoch, different samples are randomly chosen for training, while fixed samples are used during the evaluation step. Python Optimal Transport [51] is employed to implement the Sinkhorn-Knopp algorithm. The model with the best validation loss is used for augmentation and additional experiments. The hyperparameters include the learning rate, the number of layers in the backbone GNN, and the parameter  $\delta$  in Equation 5. Table 7 provides an overview of the hyperparameter search space.

Table 7: Hyperparameter search space for training the cost function.

Hyperparameter	Values
Learning rate	0.01, 0.001
# layers	2, 5
$\delta$	0.3, 0.1, 0.01

**Training vanilla model** Following the experimental setup of [4, 11, 12], we initially tune the hyperparameters related to the backbone model structure and the model training. These hyperparameters are then fixed to evaluate the performance of the augmentation methods. The hyperparameter search space for the vanilla model is provided in Table 8.

Table 8: Hyperparameter search space for training the vanilla model.

Hyperparameter	Values
Learning rate	0.01, 0.001, 0.0001
# layers	2, 5
Batch size	32, 64
Hidden dim	16, 32, 64, 128

For the TUDataset, we train the model for 100 epochs and evaluate the mean accuracy and standard deviation over five runs. In the case of the MoleculeNet dataset, we train the model for 100 epochs for the BBBP and BACE datasets and for 50 epochs for the HIV dataset. The mean AUC-ROC and standard deviation are evaluated over three runs.

**Training EPIC** During the augmentation process, a random pair of graphs is chosen as a source and target graph. One graph from the edit path between the source and target graphs is selected as the augmented data.

When evaluating the performance of EPIC, we tune two hyperparameters and select the hyperparameter combination that yields the best performance on the validation set. The augmentation ratio determines the proportion of augmented data versus the original training data. The maximum augmentation distance determines the relative maximum distance from the source to the augmented graph. A smaller maximum augmentation distance indicates that graphs closer to the source graph are sampled for augmentation. The hyperparameter search space for the EPIC is provided in Table 9.

Table 9: Hyperparameter search space for training the EPIC.

Hyperparameter	Values
Aug ratio	0.3, 0.5, 0.7
Max aug distance	0.1, 0.3, 0.5

## C Ablation Study

In this section, we describe the ablation studies conducted to configure the model structure. Specifically, we investigate the influence of different methods for determining the operation order in the edit path and the number of iterations in the Sinkhorn-Knopp algorithm.

**Ablation operation ordering** When calculating the edit distance, the specific operation order does not affect the final result. To construct the edit path, we need to determine the operation order. In our analysis, we investigate the difference between two choices of operation orders. To maintain the local connectivity of the target graph within the edit path, we employ a breadth-first search (BFS) on the target graph, and node insertion/deletion/substitution is performed following the BFS order. The results in Table 10 compare randomly ordered augmentation with BFS-ordered augmentation on eight datasets. We find no significantly better ordering choices between these two methods. To minimize additional computational overhead, we utilize random ordering for the main result.

Table 10: Comparison of randomly ordered augmentation and BFS-ordered augmentation.

	Method	NCI1	BZR	COX2	Mutagen.	IMDB-B	IMDB-M	PROTEINS	ENZYMES
GIN	BFS	81.85 <sub>(0.5)</sub>	<b>87.32</b> <sub>(1.6)</sub>	84.47 <sub>(1.8)</sub>	<b>82.09</b> <sub>(0.5)</sub>	72.80 <sub>(0.8)</sub>	48.47 <sub>(1.0)</sub>	69.69 <sub>(2.1)</sub>	<b>49.00</b> <sub>(1.8)</sub>
	Random	<b>82.31</b> <sub>(1.5)</sub>	<b>87.32</b> <sub>(2.0)</sub>	<b>84.89</b> <sub>(2.7)</sub>	81.86 <sub>(1.0)</sub>	<b>73.40</b> <sub>(0.8)</sub>	<b>48.93</b> <sub>(0.6)</sub>	<b>70.85</b> <sub>(0.9)</sub>	47.83 <sub>(3.5)</sub>

**Ablation on iterations of the Sinkhorn-Knopp algorithm** We adopt the Sinkhorn-Knopp algorithm to approximate the Hungarian algorithm to make the assignment matrix differentiable for optimization during training as described in Section 3.2. To analyze the effect of the number of iterations of the Sinkhorn-Knopp algorithm, we evaluate the classification performance under varying values of  $k$  in Equation 5. Table 11 presents the results of an ablation study.

Table 11: Classification performance under varying values of  $k$ .

Dataset	$k$										
	1	2	3	4	5	6	7	8	9	10	
GIN	BZR	87.32 <sub>(2.8)</sub>	87.07 <sub>(3.3)</sub>	88.29 <sub>(2.2)</sub>	86.34 <sub>(3.2)</sub>	86.34 <sub>(2.3)</sub>	<b>89.76</b> <sub>(2.8)</sub>	86.83 <sub>(3.7)</sub>	88.29 <sub>(2.8)</sub>	88.29 <sub>(1.1)</sub>	87.32 <sub>(1.5)</sub>
	COX2	82.98 <sub>(0.0)</sub>	84.04 <sub>(1.7)</sub>	84.04 <sub>(1.7)</sub>	84.26 <sub>(2.8)</sub>	84.04 <sub>(2.9)</sub>	83.62 <sub>(1.2)</sub>	<b>85.11</b> <sub>(1.5)</sub>	82.77 <sub>(2.2)</sub>	83.40 <sub>(2.2)</sub>	84.89 <sub>(2.7)</sub>
	IMDB-B	72.50 <sub>(0.9)</sub>	72.40 <sub>(1.2)</sub>	72.60 <sub>(0.4)</sub>	72.90 <sub>(1.1)</sub>	72.80 <sub>(1.0)</sub>	72.20 <sub>(0.8)</sub>	72.70 <sub>(0.6)</sub>	72.50 <sub>(0.4)</sub>	73.10 <sub>(0.2)</sub>	<b>73.40</b> <sub>(0.8)</sub>
	IMDB-M	48.47 <sub>(0.8)</sub>	48.33 <sub>(1.5)</sub>	48.40 <sub>(1.2)</sub>	48.67 <sub>(1.0)</sub>	47.67 <sub>(0.8)</sub>	47.80 <sub>(1.5)</sub>	48.87 <sub>(0.4)</sub>	48.33 <sub>(0.8)</sub>	<b>49.00</b> <sub>(0.5)</sub>	48.93 <sub>(0.6)</sub>
	ENZYMES	46.17 <sub>(3.1)</sub>	46.33 <sub>(3.4)</sub>	47.33 <sub>(3.1)</sub>	47.50 <sub>(4.8)</sub>	44.67 <sub>(3.9)</sub>	<b>48.17</b> <sub>(3.1)</sub>	44.33 <sub>(5.0)</sub>	43.17 <sub>(3.5)</sub>	46.00 <sub>(3.3)</sub>	47.83 <sub>(3.5)</sub>
Rank	6.4	6.2	4.4	4.4	7.0	5.6	5.2	7.2	4.0	<b>2.4</b>	

We further experiment to observe how well the assignment matrix,  $X_S$ , derived from the Sinkhorn-Knopp algorithm approximates the assignment matrix,  $X_H$ , from the Hungarian algorithm, as the parameter  $k$  varies. Firstly, we calculate both assignment matrices from our learned cost function on the test dataset and compute the Frobenius norm of the difference between the two matrices,  $\|X_A\|_F = \|X_S - X_H\|_F$ , and then, measure an average of each Frobenius norm across the entire dataset.

Figure 5 shows the average of Frobenius norm with varying  $k$ . We observe that the error decreases as  $k$  increases, suggesting that the Sinkhorn-Knopp algorithm’s assignment matrix becomes more similar to the assignment matrix from the Hungarian algorithm. However, as  $k$  increases, the computational cost required for training also increases, indicating a trade-off relationship.



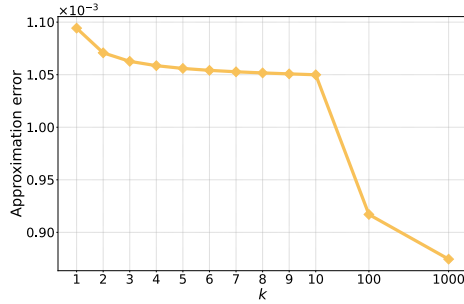


Figure 5: Frobenius norm of the difference between Hungarian algorithm’s assignment matrix and Sinkhorn-Knopp algorithm’s assignment matrix with varying  $k$  in Equation 5.

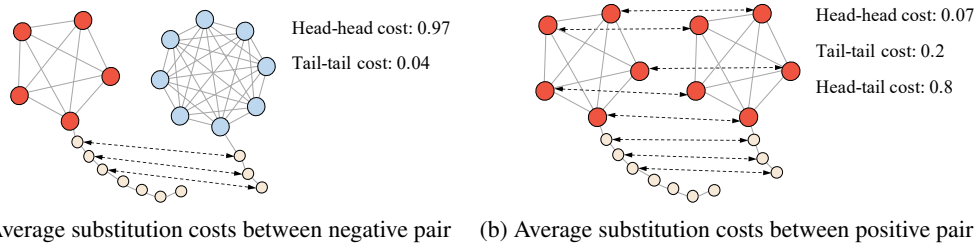


Figure 6: Analysis of substitution cost on *lollipop* graph. Normalized average substitution costs between source nodes and target nodes for *negative* pair are shown in Figure 6a and *positive* pair in Figure 6b. The costs are averaged across the entire dataset.

## D Further Analysis on *Lollipop* Dataset

To further show the effectiveness of the cost function for EPIC, we analyze the cost for substitution to each node on the *lollipop* dataset.  $(m, n)$ -*lollipop* graph consists of a head, a complete graph with  $m$  nodes, and a tail, a chain structured  $n$  nodes, with varying  $m$  and  $n$ . We use the number of heads as the label of a graph, i.e.,  $m$ . Figure 6 shows the head-to-head, head-to-tail, and tail-to-tail substitution costs. For instance, the head-to-head substitution cost measures the average substitution costs between the head nodes from the source graph with those of the target graph.

With the *negative pair*, the average node substitution cost for the head nodes is 0.97, whereas the average for the tail nodes is 0.04. These results align with our intuition that editing the head, closely related to the label, incurs a high cost. Thus, any modification to this part leads to substantial changes in the label. With the *positive pair*, the head-to-head and tail-to-tail substitution costs are 0.07 and 0.2, respectively. Those values are much smaller than 0.8 of head-tail costs. The lower cost for the head-head substitution in a positive pair resulted from the fact that it involves the exchange of nodes associated with the same label. Similarly, the low cost for the tail-to-tail substitution aligns well with our intuition since the nodes are unrelated to the label. In contrast, the head-to-tail substitution is assigned a high cost because it substitutes a label-associated part with a non-associated part. This preserves the head part of every graph on the edit path between *positive*-pair, ensuring that the augmented graph keeps the same label over the path.

## E Examples of Edit Path

Figure 7 and Figure 8 illustrate examples of the edit path generated by EPIC on the IMDB-BINARY dataset and PROTEINS dataset, respectively. In each figure, the upper left graph with blue nodes represents the source graph, and the lower right graph with red nodes represents the target graph.

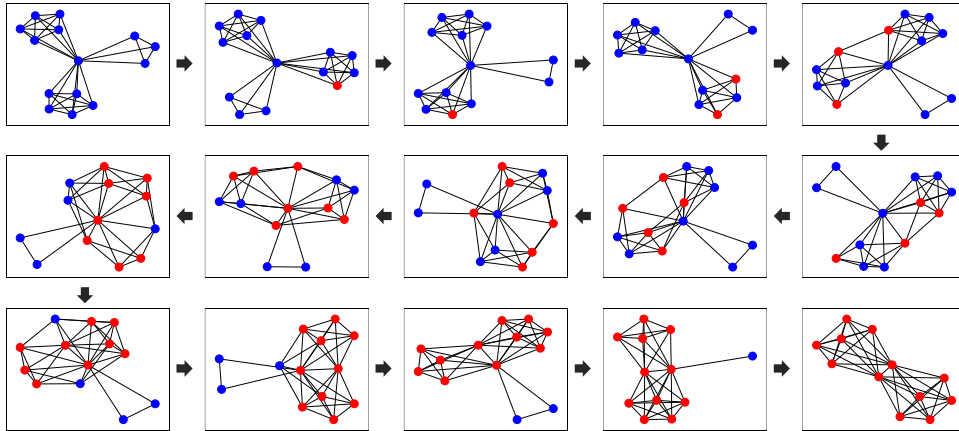


Figure 7: The example of the edit path generated by EPIC on the IMDB-BINARY dataset.

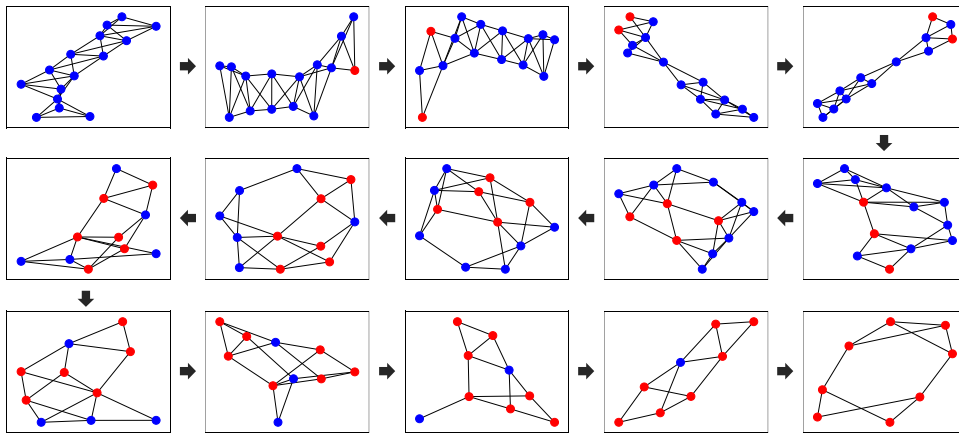


Figure 8: The example of the edit path generated by EPIC on the PROTEINS dataset.